Int. J. Heat Mass Transfer. Vol. 21, pp. 1167–1170

0017-9310/78/0801-1167 $02.00/0

SHORTER COMMUNICATIONS

TURBULENT BOUNDARY-LAYER TEMPERATURE PROFILES AND REYNOLDS ANALOGY

R. E. WILSON*
Naval Surface Weapons Center, Dahlgren Laboratory, Dahlgren, Virginia 22448, U.S.A.

(*Received* 4 *April* 1977)

NOMENCLATURE

- r, temperature recovery factor;
- S, Reynolds analogy factor;
- Pr, laminar Prandtl number;
- Λ, ratio of thermal-to-velocity boundary-layer thickness;
- T, absolute temperature;
- T_r, recovery temperature;
- ρ, density;
- γ, ratio of specific heats, c_p/c_v;
- c_p, specific heat at constant pressure;
- c_v, specific heat at constant volume;
- x, distance along flat plate, measured from leading edge;
- u, velocity in x direction;
- M, Mach number based on u;
- δ, velocity boundary-layer thickness;
- n, exponent in power law approximation of velocity profile;
- St, mean Stanton number;
- C_F, mean skin friction coefficient.

Subscripts

- w, conditions at surface of the plate;
- l, conditions at boundary-layer edge;
- T, stagnation conditions.

IN 1942, Squire [1] postulated a flat-plate turbulent boundary-layer temperature profile for zero heat transfer and Prandtl numbers different from unity. This profile is similar to the Prandtl number unity profile but incorporates the recovery factor, r, and the ratio of thermal-to-velocity boundary-layer thickness, Λ. Assuming a power-law velocity profile, he deduced that the recovery factor was related to the laminar Prandtl number, Pr, by $r = Pr^{1/3}$. In this note Squire's profile has been extended to cover finite heat transfer. Again, the profile is similar to the Prandtl number unity profile but incorporates r and Λ. Using this profile, an expression for the Reynolds analogy factor, S, has been deduced for turbulent flow. The expression, $S = 1/r = Pr^{-1/3}$, agrees with experiment (within the scatter of the data) over a wide range of Mach numbers. In addition, the postulated temperature profiles exhibit much the same features as measured profiles.

RESULTS AND DISCUSSION

For zero heat transfer with both laminar and turbulent Prandtl numbers equal to unity, the boundary-layer temperature on a flat-plate is given by

$$\frac{T}{T_1} = 1 + \frac{\gamma-1}{2} M_1^2 \left[1 - \left(\frac{u}{u_1}\right)^2\right] \tag{1}$$

where the subscript "1" represents freestream conditions. For Prandtl numbers other than unity, Squire [1] assumed the following expression had a certain plausibility

$$\frac{T}{T_1} = 1 + r\frac{\gamma-1}{2} M_1^2 \left[1 - g^2\left(\frac{y}{\Lambda}\right)\right] \tag{2}$$

where

$$\left.\begin{aligned} &\frac{u}{u_1} = g(y) \\ &y = 0,\ g(y) = 0;\quad y \geqslant \delta,\ g(y) = 1 \\ &y = 0,\ g\left(\frac{y}{\Lambda}\right) = 0;\quad y \geqslant \Lambda g,\ g\left(\frac{y}{\Lambda}\right) = 1. \end{aligned}\right\} \tag{3}$$

At $y = 0$, equation (2) gives the recovery temperature, T_r. Using equation (2) and satisfying the boundary-layer energy equation at the wall, Squire obtained

$$r = Pr\Lambda^2. \tag{4}$$

For turbulent boundary-layers, a familiar approximation for the velocity distribution is

$$\left.\begin{aligned} &\frac{u}{u_1} = \left(\frac{y}{\delta}\right)^{1/n}, \quad 0 \leqslant y \leqslant \delta \\ &\frac{u}{u_1} = 1, \qquad\quad y \geqslant \delta \end{aligned}\right\} \tag{5}$$

where n is about 7. Squire made use of equations (2) and (5) in satisfying the condition that the energy deficit across the boundary-layer must be zero for zero heat transfer. From this condition, at Mach numbers less than one half and values of Λ less than unity, he obtained

$$r\Lambda^{(n+1)/n} = 1. \tag{6}$$

This result also holds for values of Λ greater than but near unity. Combining equations (4) and (6) yields

$$r = Pr^{(n+1)/(3n+1)}. \tag{7}$$

For pertinent values of $n (n > 5)$ and for Pr not very different from unity ($Pr = 0.7$–1.3), the following is sufficiently accurate.

$$r = Pr^{1/3}. \tag{8}$$

Although this result was derived for low Mach numbers, with perfect gas conditions equation (8) is a good approximation to experimental data for a wide range of Mach numbers [2].

Now with finite heat transfer and both laminar and turbulent Prandtl numbers equal to unity, the boundary-layer temperature from [3] can be written as

$$\frac{T}{T_1} = 1 - \left(1 + \frac{\gamma-1}{2} M_1^2 - \frac{T_w}{T_1}\right)\left(1 - \frac{u}{u_1}\right) + \frac{\gamma-1}{2} M_1^2 \left[1 - \left(\frac{u}{u_1}\right)^2\right] \tag{9}$$

*Head, Weapons Systems Department.

where T_w is the wall temperature. This equation can readily be reduced to the familiar Crocco [4] expression

$$\frac{T_T - T_w}{T_{T1} - T_w} = \frac{u}{u_1} \tag{10}$$

where the total temperature, T_T, is given by

$$T_T = \left(1 + \frac{\gamma - 1}{2} M^2\right) T.$$

For Prandtl numbers other than one, it seems reasonable to extend Squire's assumption for zero heat transfer by writing

$$\frac{T}{T_1} = 1 - \left(1 + r\frac{\gamma - 1}{2} M_1^2 - \frac{T_w}{T_1}\right)\left[1 - g\left(\frac{y}{\Lambda}\right)\right] + r\frac{\gamma - 1}{2} M_1^2\left[1 - g^2\left(\frac{y}{\Lambda}\right)\right]. \tag{11}$$

For the case of zero heat transfer, Squire set the energy deficit across the boundary-layer equal to zero and derived equation (6). With finite heat transfer, the energy deficit across the boundary-layer can be related to the skin friction drag using Reynolds' analogy as follows. The heat transfer, Q, and skin friction drag, D, for fully developed turbulent flow on a flat-plate of length x are given by

$$Q = \int_0^\infty \rho u c_p (T_{T1} - T_T)\,dy = \rho_1 u_1 c_p St (T_r - T_w) x \tag{12}$$

$$D = \int_0^\infty \rho u (u_1 - u)\,dy = \rho_1 u_1^2 \frac{C_F}{2} x. \tag{13}$$

With the Reynolds' analogy factor relating the mean Stanton number, St, and mean friction coefficient, C_F, by

$$S = \frac{2St}{C_F} \tag{14}$$

and the density, ρ, given by

$$\rho = \frac{T_1}{T}\rho_1. \tag{15}$$

Equations (12) and (13) can be combined to yield

$$\int_0^\infty \frac{u}{T}(T_{T1} - T_T)\,dy = \frac{S(T_r - T_w)}{u_1}\int_0^\infty \frac{u}{T}(u_1 - u)\,dy. \tag{16}$$

Equation (16) can be used to determine the Reynolds' analogy factor. This is accomplished by approaching the condition of zero heat transfer and zero Mach number along two separate paths. Take Λ less than unity, the power law velocity profile, and first put $T_w = T_r$ for zero heat transfer in equation (16). With the temperature given by equation (11), as $M_1 \to 0$ the relation between r and Λ given by equation (6) results. Now first put $M_1 = 0$ in equation (16), then as $T_w \to T_r$ the following result is obtained

$$S = \Lambda^{(n+1)/n}. \tag{17}$$

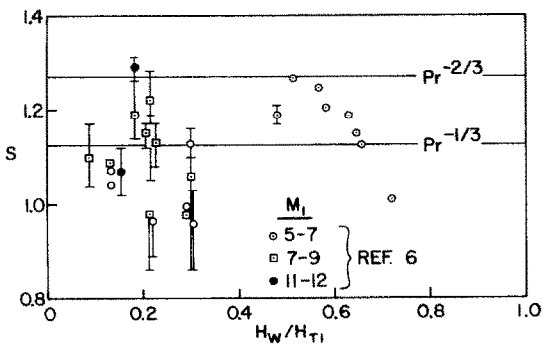

FIG. 1. Reynolds analogy factor.

As in the case of equation (6), this result holds for Λ greater than but near unity. Combining equations (6) and (17),

$$S = \frac{1}{r}. \tag{18}$$

As already stated, the expression for recovery factor given by equation (8), $r = Pr^{1/3}$, is in good agreement with experiment over a wide range of Mach numbers. Taking $Pr = 0.7$ as a representative value for laboratory experiments, equation (18) yields $S = Pr^{-1/3} = 1.13$. Chi and Spalding [5] computed S from measured local heat-transfer coefficients and computed values of local skin friction coefficient. For two-dimensional plane and axisymmetric zero pressure gradient flows at Mach numbers less than 5 and wall to total temperature ratios from 0.5 to 1.12, they concluded Mach number and heat transfer had no apparent effect on S. A value of $S = 1.16$ provided the best fit to the data. This is in excellent agreement with the value of 1.13 from equation (18). Flat plate data at Mach numbers from 5 to 12 and wall to total enthalpy ratios from 0.1 to 0.7 were collected by Cary [6]. The values of S he deduced from simultaneous measurements of local heat transfer and skin friction are presented on Fig. 1. A temperature recovery factor of 0.89 was used in reducing the data. Although there is considerable scatter in the data, $S = Pr^{-1/3}$ gives a very reasonable mean value. For comparison, the value $S = Pr^{-2/3}$ for laminar boundary-layer flow is also shown on Fig. 1. As several authors have noted, this value is too high to be representative for turbulent boundary-layer flow.

With $r = Pr^{1/3}$ and $S = Pr^{-1/3}$, equation (16) can now be solved numerically to determine the variation of Λ with Mach number and wall temperature. The boundary-layer temperature is given by equation (11) and a power law velocity distribution is assumed. Figure 2(a) first shows the sensitivity of Δ to n and Mach number at zero heat transfer. Figure 2(b) shows the effect of wall temperature and Mach number with $n = 7$.

With values of r and Λ determined, the accuracy with which equation (11) represents experimental temperature profiles can be examined. For power law velocity profiles, equation (11) can be written

$$\frac{T_T - T_w}{T_{T1} - T_w} = \Lambda^{-1/n}\left(\frac{T_r - T_w}{T_{T1} - T_w}\right)\frac{u}{u_1} + \left\{\frac{T_{T1} - T_1}{T_{T1} - T_w} - \Lambda^{-2/n}\left(\frac{T_r - T_1}{T_{T1} - T_w}\right)\right\}\left(\frac{u}{u_1}\right)^2. \tag{19}$$

With values of Λ from Fig. 2(b) and $r = Pr^{1/3}$, temperature as a function of velocity can be computed from equation (19) for given Mach numbers and wall temperatures. On Figs. 3(a)–(c) computed values are compared with data from Bertram and Neal [7] on a hollow cylinder of constant diameter. Flat plate measurements by Danberg [8] are

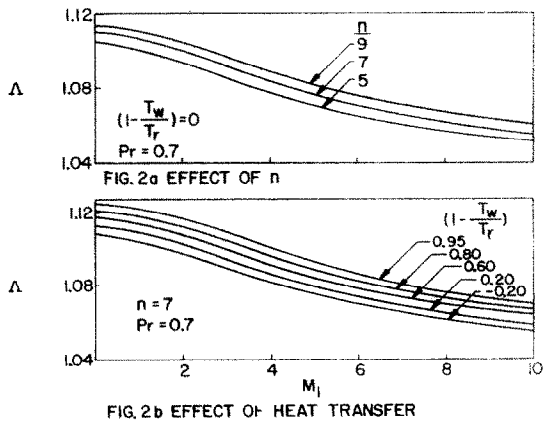

FIG. 2. Ratio of thermal-to-velocity boundary thickness.

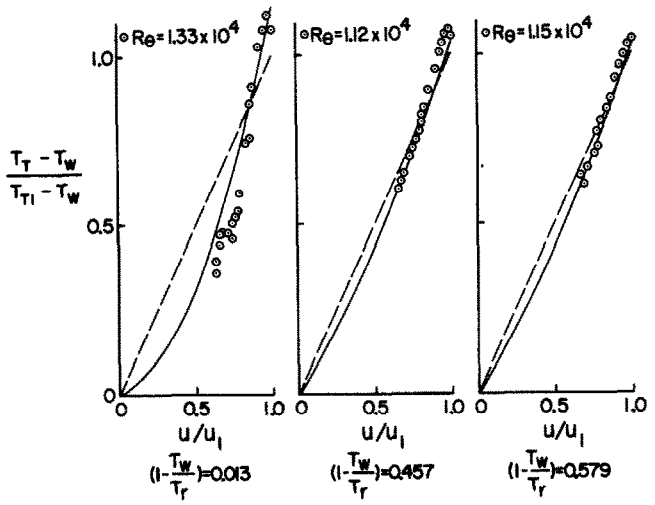

FIG. 3. Comparison of temperature profiles, $M_1 = 6.0$. —— equation (19), $Pr = 0.7$; --- Crocco; ⊙ Bertram and Neal.

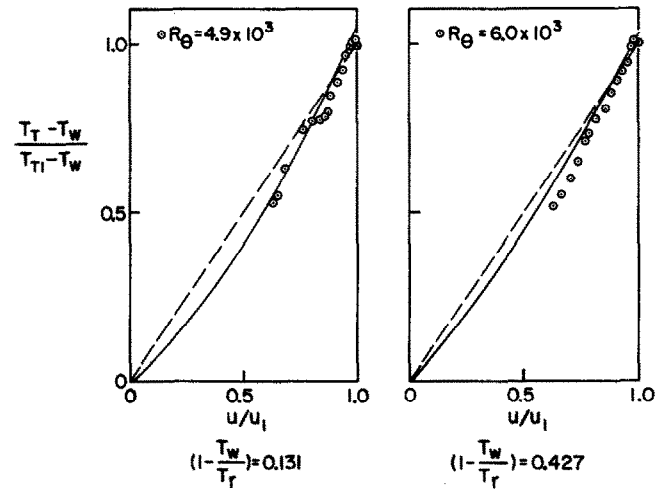

FIG. 4. Comparison of temperature profiles, $M_1 = 6.3$. —— equation (19), $Pr = 0.7$; --- Crocco; ⊙ Danberg.

compared with computation on Fig. 4. The data from both sources are for two-dimensional flow at constant wall temperature and pressure. These data were selected for the comparison rather than nozzle wall experiments where variations in pressure and wall temperature greatly affect the results. For the momentum thickness Reynolds' numbers, R_θ, associated with the data, transition was well upstream of the survey station. The measurements were thus made in fully developed turbulent flow.

Comparison with experiment demonstrates that equation (19) produces temperature profiles which have much the same features as measured profiles. At lower velocities the temperature falls below the prediction of Crocco given by equation (10). At the outer edge of the boundary layer the temperature overshoots Crocco's prediction. As the wall temperature is reduced and heat transfer increases, both equation (19) and experiment come closer to the Crocco profile. However, there are differences between equation (19) and experiment. A comparison of Figs. 3 and 4 with values of $[1-(T_w/T_r)]$ of 0.457 and 0.427, respectively, suggest this may, in part, be due to the difficulty in making accurate temperature measurements. The data on the two figures were obtained under very similar conditions and should check. It can be seen the results from the two sources are significantly different. Note that the data fall above equation (19) on Fig. 3 and below equation (19) on Fig. 4.

It should be noted that the postulated temperature profile cannot be expected to give accurate results near the wall. There the molecular shear stress becomes important and the details of transition from the laminar sublayer to the fully turbulent part of the boundary layer must be considered [9].

REFERENCES

1. H. B. Squire, Heat transfer calculations for aerofoils, Ministry of Aircraft Production, London, R & M No. 1986 (November 1942).
2. R. E. Wilson, *Handbook of Supersonic Aerodynamics*, Sections 13 and 14 Viscosity and heat transfer effects, NAVORD Report 1488, Vol. I, p. 193. U.S. Government Printing Office, Washington (August 1966).
3. C. C. Tin, Turbulent flows and heat transfer, in *High Speed Aerodynamics and Jet Propulsion*, Vol. 5, p. 91. Princeton University Press, Princeton, New Jersey (1959).
4. L. Crocco, The laminar boundary layer in gases, North American Aviation, Inc., Los Angeles, California, APL/NAA/CF-1038 (July 1948).
5. C. S. Chi and D. B. Spalding, Influence of temperature ratio on heat transfer to a flat plate through a turbulent

boundary layer in air, in *Proceedings of the Third International Heat Transfer Conference*, Vol. 2, p. 41–49. A.I.C.E., New York (1966).
6. A. M. Cary, Jr., Summary of available information on Reynolds' analogy for zero-pressure-gradient, compressible, turbulent-boundary-layer flow, National Aeronautics and Space Administration, Washington, D.C., NASA TN D-5560 (January 1970).
7. M. H. Bertram and L. Neal, Jr., Recent experiments in hypersonic turbulent boundary layers, National Aeronautics and Space Administration, Washington, D.C. NASA TMX56335. Presented at the AGARD Specialists Meeting on Recent Developments in Boundary Layer Research, Naples, Italy (10–14 May 1965).
8. J. E. Danberg, Characteristics of the turbulent boundary layer with heat and mass transfer at $M = 6.7$, U.S. Naval Ordnance Laboratory, White Oak, Maryland, NOL TR 64-99 (October 1964).
9. H. U. Meier, R. L. P. Voisinet and D. F. Gates, Temperature distributions using the law of the wall for compressible flow with variable turbulent Prandtl numbers, AIAA Paper No. 74-596, presented at the AIAA 7th Fluid and Plasma Dynamics Conference at Palo Alto, California (17–19 June 1974).

Int. J. Heat Mass Transfer. Vol. 21, pp. 1170–1171

0017-9310/78/0801-1170 $02.00/0

A STEP-BY-STEP METHOD FOR THE CALCULATION OF THE CONCENTRATION DEPENDENCE OF THE DIFFUSION COEFFICIENT FROM A SINGLE (DE)SORPTION EXPERIMENT

WILLEM J. A. H. SCHOEBER† and HANS A. C. THIJSSEN
Eindhoven University of Technology, Department of Chemical Engineering, P.O. Box 513, Eindhoven, The Netherlands

(*Received 2 February* 1977)

NOMENCLATURE

- a_i, activity of the sorbent;
- D_i, diffusion coefficient [m^2/s];
- J, mass flux [$kg/m^2 s$];
- k_c, continuous phase mass-transfer coefficient [m/s];
- m_i, mass concentration [kg/m^3];
- n, number of intervals;
- t, time [s];
- z, distance coordinate [m];
- Δt, time interval [s];
- ρ_{bulk}, mass concentration of sorbent in the bulk of the continuous phase [kg/m^3];
- ρ^*_{pure}, mass concentration of sorbent in the continuous phase in equilibrium with pure sorbent at the temperature of the dispersed phase [kg/m^3].

Subscripts

- i, at the interface between dispersed and continuous phase;
- cr, at the critical point;
- 0,1,2,3, indicate limits of concentration intervals.

INTRODUCTION

THE CONCENTRATION dependence of a diffusion coefficient can be obtained from a number of successive experiments at different concentration levels [1] or by interpretation of a single (de)sorption experiment. Some methods of the latter type require the assumption of a certain functional relation between diffusivity and concentration [2, 3]. Duda and Vrentas [4] developed a method in which such an assumption is not necessary. It makes use of an approximate solution of the diffusion equation for constant surface concentration. The present method which has been described by Schoeber [5] deals with diffusion with variable surface concentration. It shows some similarity to Prager's method [6] for the interpretation of successive sorption experiments.

APPROACH

In a (de)sorption experiment the surface flux is measured as a function of time. The surface concentration in the dispersed phase is calculated from the equation describing the sorption flux in the continuous phase:

$$J = k_c(a_i \rho^*_{pure} - \rho_{bulk}). \quad (1)$$

All variables in this equation can be measured experimentally except a_i, which can therefore be calculated from this equation. The sorption isotherm, i.e. the relation between the surface concentration m_i and the surface activity a_i, will then reveal the value of m_i.

In the present method we adopt a step-function approximation to the concentration dependence of the diffusion coefficient. The diffusion coefficient in a concentration interval $m_{j-1} > m > m_j$ is assumed to be constant and to be the value of D_j.

Successive concentration profiles during a desorption process, starting at a homogeneous initial concentration m_0, are drawn schematically in Fig. 1. In this example the system does not shrink upon desorption. After time t_1 the surface concentration equals m_1. By application of a single parameter estimation to the solution of the diffusion equation the diffusivity D_1 can be calculated from the experimental data. At time t_2 the surface concentration has reached m_2. Over the interval $m_1 < m < m_2$ the corresponding value of the diffusion coefficient, D_2, can now be calculated. In this calcu-

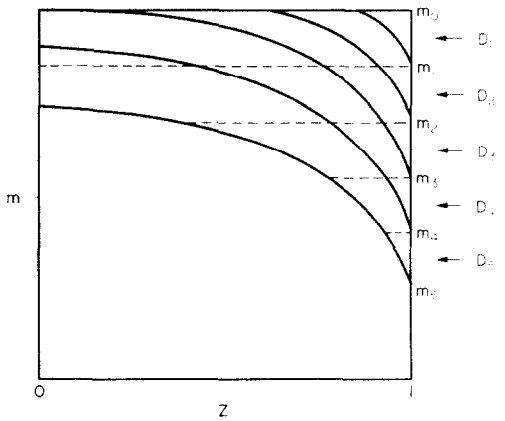

FIG. 1. Schematic representation of the change in concentration profile during a desorption process.

†Present address: Koninklyke/Shell Laboratorium Amsterdam, P.O. Box 3003, Amsterdam, The Netherlands.